



Assessing the Impact of Modified Initial Abstraction Ratios and Slope Adjusted Curve Number on Runoff Prediction in the Watersheds

Farhan Ahmad Abdulrahman ^{a*} , Tariq Hama Karim ^b ^a Department of Soil and Water, College of Agricultural Engineering Sciences, Salahaddin University, Erbil, Iraq.^b Department of Survey and Geomatics Engineering, Faculty of Engineering, Tishk International University, Erbil, Iraq.

Submitted: 27 April 2024

Revised: 15 May 2024

Accepted: 23 May 2024

*Corresponding Author:

farhan.abdulrahman@student.su.edu.krd

Keywords: Runoff estimation, SCS-CN method, Slope adjusted CN, Initial abstraction ratio, Sulaimani watersheds.**How to cite this paper:** F. A. Abdulrahman and T. H. Karim, "Assessing the Impact of Modified Initial Abstraction Ratios and Slope Adjusted Curve Number on Runoff Prediction in the Watersheds of Sulaimani Province", *KJAR*, vol. 9, no. 1, pp. 77-92, Jun. 2024, [doi: 10.24017/science.2024.1.7](https://doi.org/10.24017/science.2024.1.7).

Copyright: © 2024 by the authors. This article is an open access article distributed under the terms and conditions of the Creative Commons Attribution (CC BY-NC-ND 4.0)

Abstract: The curve number (CN) method is widely recognised as a valuable tool for assessing the correlation between storm rainfall depth and direct runoff. Despite its simplicity, extensive research, and widespread application, the influence of slope and the initial abstraction ratio (λ) on direct runoff, particularly when employing the soil conservation service-curve number (SCS-CN) method, has not received adequate attention. Accurate predictions necessitate accounting for these critical variables. Traditionally, the initial abstraction ratio (λ) has been assumed to be 0.20, in line with the original recommendations of the method's developers. This study scrutinised daily precipitation data from seventeen watersheds across diverse physiographic regions within Iraq's Kurdistan region, collected between 2022 and 2023. The objective was to evaluate the impact of adjusting the CN for slope and modifying the initial abstraction ratio ($\lambda = 0.1$) on direct runoff estimation. Findings revealed that incorporating slope adjustments and employing a revised initial abstraction ratio resulted in more precise runoff predictions compared to the conventional method, which neglected slope and utilised $\lambda = 0.2$. Therefore, in the application of the SCS-CN approach, it is essential to adjust the CN for slopes in mountainous areas and consider the initial abstraction ratio, rather than solely relying on the standard value of 0.2. This study underscores the significance of accounting for local conditions and determining the initial abstraction ratio based on watershed-specific characteristics to enhance the accuracy of direct runoff estimation using the CN method.

1. Introduction

In 1954, the Soil Conservation Service, now the Natural Resources Conservation Service (NRCS), of the US Department of Agriculture created the Soil Conservation Service-Curve Number (SCS-CN) method, an empirical lumped rainfall-runoff model [1]. The scientific community widely accepts this model for predicting direct runoff from watersheds during specific rainfall events due to its simplicity and minimal data requirements [1, 2]. It integrates various variables such as antecedent runoff condition, soil group, surface condition, land cover, and land use into a single curve number (CN) parameter [3]. However, using tabulated CN values often leads to over-building of hydrological systems, overstating initial abstraction (Ia) and potential maximum retention [4, 5].

There are limitations across different geographic areas, and doubts have been raised about the reliability of the assumed constant value of 0.2 for the initial abstraction ratio (λ) [6]. Various factors

related to rainfall events and landscape characteristics have been investigated to estimate a suitable value for λ , leading to uncertainties and re-evaluations [6-11]. It has been suggested that λ should be considered region-specific, as the ideal value may differ depending on the geographical area or region [12]. A study in the Czech Republic investigated five watersheds to estimate discharge [13].

Eventually, researchers discovered that the standard SCS-CN method was inadequate, necessitating adjustments to the parameters of λ and CN to achieve suitable and acceptable direct runoff values across all watersheds under investigation. While CN values require greater flexibility as they represent catchment-dependent parameters, it was concluded that λ must be less than 0.2 for more accurate results. Utilising an asymptotic fitting approach, one study [14] demonstrated that decreasing the value of λ to 0.05 resulted in improved accuracy of predictions. Several investigators, particularly those cited in references [9-11], have advocated for modifying λ to 0.05 based on their findings, proposing this adjustment as a more appropriate value for enhancing the model's predictive accuracy in practical applications. Another study [15] proposed an optimal value of $\lambda = 0.15$ based on their analysis.

In a recent investigation [16], the λ was studied in three watersheds located in the Halabja governorate of the Kurdistan region, revealing a λ value around 0.1, which is below 0.2. The original design of the NRCS model focused on agricultural watersheds with land slopes of 5% or less, thus neglecting the influence of slope when estimating runoff. However, subsequent research has re-examined runoff estimation in relation to watershed slope [17-19]. Slope-adjusted CN can enhance the NRCS model's runoff estimation capacity, as steeply sloped watersheds experience increased runoff due to reduced depression storage and ponding depth [20]. Studies have shown that as slope increases, there is a significant rise in runoff depth, with one study [17] reporting a 10% increase in runoff depth in pastures and a 23% increase in alfalfa for each incremental rise in slope. Additionally, employing the Huang *et al.* (2006) equation, another study [21] in the Kardeh watershed (Iran) established a direct correlation between measured and predicted runoff depths, highlighting the efficacy of the slope-adjusted CN approach [22] over the conventional tabulated CN method. This study aims to explore the impact of the adjusted λ and slope-adjusted CN on runoff estimation

2. Materials and Methods

2.1. Study Area Description

This study utilised a database comprising seventeen watersheds situated in the Sulaimani governorate of the Iraqi Kurdistan Region, as delineated in figures 1 and 2. These watersheds exhibit varying sizes, with WS11 encompassing an area of 24.33 km² and WS8 is extending over an area of 254.18 km². They are geographically situated between longitudes 44° 00' E and 46° 30' E and latitudes 34° 30' N and 37° 00' N. As per the digital elevation model (DEM), the elevations within the study area range from 196 to 3152 meters above mean sea level. The average slopes of the watersheds vary, ranging from 5.94% for WS1 to 47.67% for WS17, as illustrated in table 1. In terms of climate classification, Koppen's scheme designates all the watersheds as falling under the Csa class. This climate category, typical of Mediterranean regions, is characterised by cold, rainy winters and hot, dry summers. The study area experiences an average annual precipitation of 228 mm in the south and southwest and 1350 mm in the north and northeast, based on historical rainfall data collected at meteorological stations over a 23-year period (2001-2023). The majority of the rainfall is concentrated between October and May.

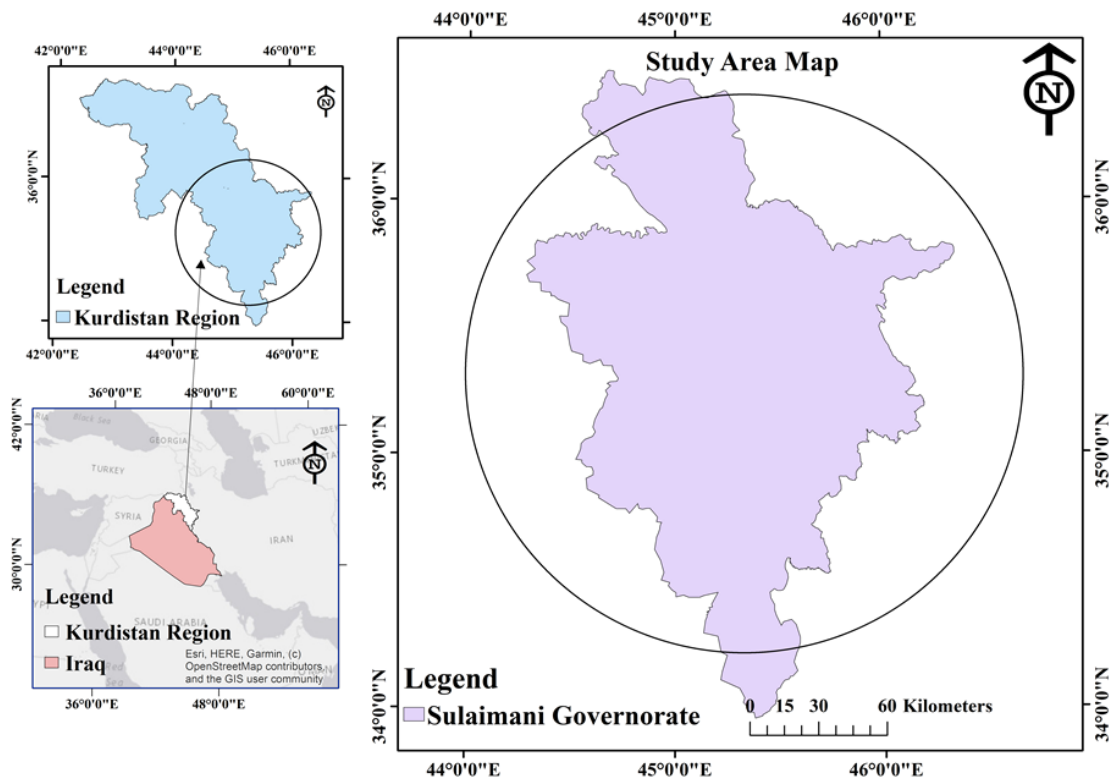


Figure 1: Study area location map.

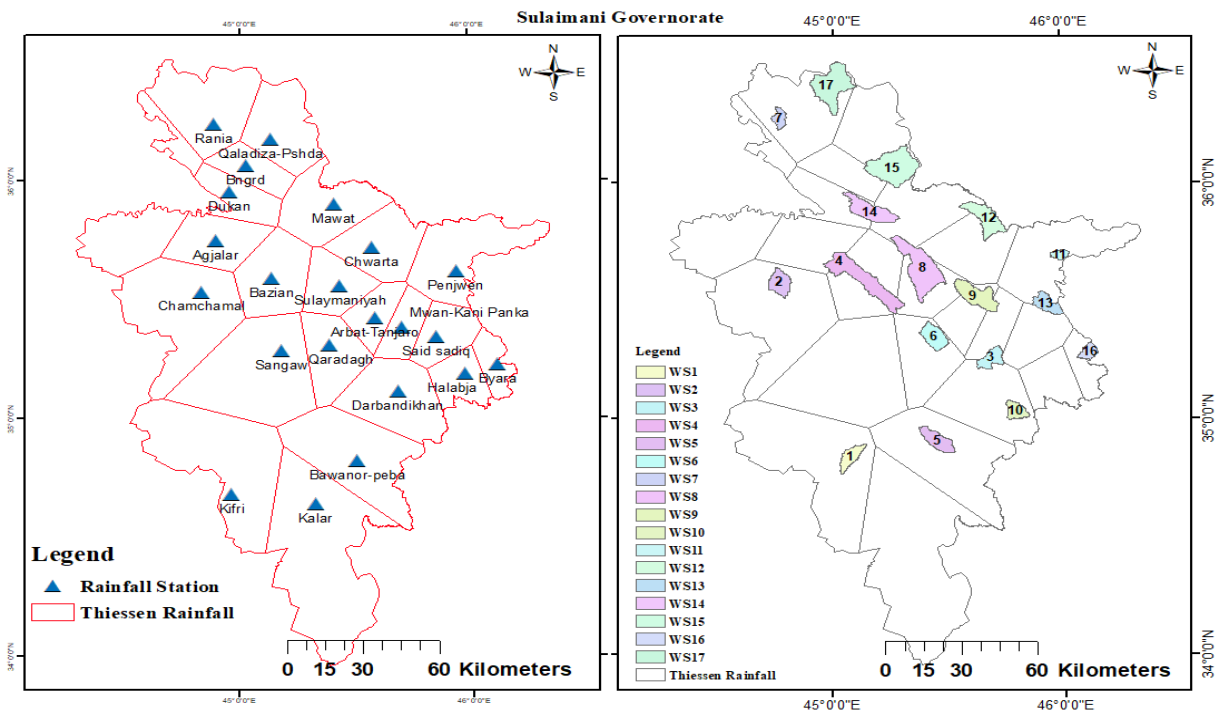


Figure 2: Location map showing the meteorological station and watersheds.

Table 1: Description of watersheds under study

No.	Watershed	Watershed code	Outlet coordinates		Area (km ²)	Slope (%)
			Latitude	Longitude		
1	Rizgary	WS1	34°46'24.8"	45°02'03.3"	64.72	5.94
2	Qarahanjir	WS2	35°35'07.3"	44°43'00.4"	80.91	7.86
3	Kanikawa	WS3	35°18'44.9"	45°43'34.7"	66.82	12.85
4	Bazyan	WS4	35°31'50.9"	45°09'44.6"	236.29	15.34
5	Pebaz	WS5	34°51'53.7"	45°31'48.3"	86.43	18.83
6	Qaradagh	WS6	35°17'27.2"	45°27'33.3"	88.14	19.61
7	Betwata	WS7	36°13'49.2"	44°45'09"	36.84	23.60
8	Awal	WS8	35°29'43.2"	45°23'24.1"	254.18	23.64
9	Barznja	WS9	35°35'53.5"	45°32'52.8"	137.29	24.82
10	Darbandikhan	WS10	35°01'01"	45°51'17.8"	54.69	27.70
11	Penjwen	WS11	35°41'20.8"	45°57'18.8"	24.33	27.74
12	Sewail	WS12	35°45'33.5"	45°39'46.2"	131.17	41.74
13	Chawtan	WS13	35°29'19.6"	45°52'29.2"	69.23	44.71
14	Surdash	WS14	35°58'00.1"	45°04'26.5"	137.01	45.13
15	Bngrd	WS15	36°06'12.1"	45°10'24.1"	244.06	45.56
16	Gulp	WS16	35°15'35.4"	46°03'47.2"	37.76	45.91
17	Sangasar	WS17	36°17'34.4"	45°00'28.5"	209.61	47.67

2.2. Preparation of Rainfall Maps

Meteorological data spanning the periods 2021-2022 and 2022-2023 were sourced from meteorological stations situated across the study area. Employing the Thiessen Polygon method, precipitation maps were generated using ArcGIS. Originating from Thiessen in 1911, the Thiessen method accounts for the spatial weighting of areas by assigning the closest polygon to each station. Its primary objective is to mitigate errors arising from the non-uniform distribution of rain gauges. This approach delineates Thiessen polygons to demarcate the coverage area effectively.

2.3. SCS-CN Method

2.3.1. Estimation Runoff by the SCS-CN Method

The SCS-CN method, pioneered by the Soil Conservation Service (SCS) in 1972, comprises a set of mathematical equations. These equations rely on input data related to land covers, land use patterns, soil hydrology, vegetation types, and rainfall quantities. These assumptions can be delineated individually as follows:

$$P = Ia + F + Q \quad (1)$$

$$\frac{Q}{P-Ia} = \frac{F}{S} \quad (2)$$

$$Ia = \lambda S \quad (3)$$

The SCS-CN method integrates various equations to derive the equation for direct runoff (Q). To formulate these equations accurately, essential parameters such as Q in millimetres, precipitation (P) in millimetres, Ia in millimetres, cumulative infiltration minus initial abstraction (F), potential maximum retention after the start of runoff (S) in millimetres, and λ are required. Through the process of integration applied to these equations, we can obtain the exact mathematical expression for the variable Q.

$$Q = \frac{(P-\lambda S)^2}{P+(1-\lambda)S} \quad (4)$$

Eq. (4) is valid for $P < I_a$, and $Q = 0$. The S value has a direct correlation with CN and can range from 0 to infinity. According to previous study [23], the CN value can be utilised for parameter S in the following manner:

$$S = \frac{25400}{CN} - 254 \quad (5)$$

The initial abstraction ratio (λ) was not initially considered in the development of the SCS-CN method. However, as the method evolved, λ was included by assuming a constant value for the ratio of I_a to potential maximum retention (S). According to NEH-4 (SCS, 1985), approximately 50% of the gathered data points fell within the range of 0.095 to 0.38. Consequently, a standardised value of λ was established at 0.2 [12].

So, Equation (3) changes into:

$$I_a = 0.2S \quad (6)$$

This changes Equation (4) into:

$$Q = \frac{(P-0.2S)^2}{P+0.8S} \quad (7)$$

In order to assess the impact of the initial abstraction ratio on the predicted runoff, we modified the value of the initial abstraction ratio to $\lambda=0.1$, as proposed by Abdulrahman and Karim [16] in their examination of three watersheds within the Halabja governorate region. Subsequently, we employed this adjusted ratio to estimate the runoff quantity for all the watersheds under investigation.

2.3.2. Soil Hydrologic Group of the Study Watersheds

The classification of soil based on its infiltration and runoff capability entails the use of four hydrological groups [24]: A, B, C, and D.

- Group (A) encompasses soil types characterised by high rates of infiltration, typically falling within the range of 8–12 mm per hour, coupled with a low propensity for runoff.
- Group (B) comprises soils with a moderate level of infiltration, typically ranging from 4 to 8 mm per hour, and exhibiting a moderately low potential for runoff.
- Soils classified under Group (C) demonstrate a relatively slow rate of water infiltration, typically ranging from 1 to 4 mm per hour, and display a somewhat heightened tendency for runoff.
- In contrast, group (D) soils exhibit minimal infiltration capacity, generally ranging from 0 to 1 mm per hour, rendering them highly susceptible to runoff.

2.3.3. Antecedent Moisture Condition

The term "antecedent moisture condition" (AMC) pertains to the soil moisture level existing five days prior to a precipitation occurrence. Adjustments to the CN are made based on the prevailing season and soil conditions, resulting in either (CNI OR CNIII) for dry or wet condition, respectively. Determining the suitable AMC class involves evaluating the cumulative precipitation accumulated over the preceding five-day period. In this research, we adopted AMCII to derive CNII. The delineations for these AMC categories are outlined in table 2 as previously reported [25].

Table 2: Antecedent moisture conditions groups.

AMC Group	Total Rainfall Depth in the Previous 5 Days (mm)	
	Dormant Season	Growing Season
I	Less than 12.7	Less than 35.6
II	12.7-28	35.6-53.4
III	More than 28	More than 53.4

2.3.4. Land Use and Land Cover (LULC)

This characteristic denotes the land utilisation pattern or the constitution of the uppermost soil layer. When referencing tables containing CN values, they should encompass details regarding land use/land cover and the condition of the surface soil layer in hydrological terms. These tables furnish the CN values for AMCII (also referred to as CNII) based on land use and land cover. However, adjustments to the CN in these tables become necessary if incorporating the AMC classification into either the most recent group III or the earliest group I. Equation (8) allows for the conversion of CNII to CNI, while equation (9) facilitates the conversion of CNII to CNIII [26].

$$CN_I = \frac{CN_{II}}{2.2754 - 0.012754CN_{II}} \quad (8)$$

$$CN_{III} = \frac{CN_{II}}{0.430 - 0.0059CN_{II}} \quad (9)$$

2.4. Data Acquisitions

We have prepared the downloaded spatial dataset for processing, summarising it as follows:

1. The DEM with a resolution of 30 meters was provided by the United States Geological Survey and NASA Earth Data.
2. The Environmental Systems Research Institute (ESRI) supplied the land use and land cover dataset for the study area. The website <https://livingatlas.arcgis.com/landcover/> was available. Utilising observations from over 2,000,000 global sources across six spectral bands with a spatial resolution of 10 meters, we generated a detailed map. These observations were collected by the high-resolution Sentinel-2 satellite, which conducted annual surveys from 2017 to 2021.
3. Access to the Harmonised World Soil Database (HWSD) was granted by the United States' International Food and Agriculture Organisation (FAO). The HWSD provides a raster database of soil data with a spatial resolution of 30 arc seconds. The soil data grid and viewer can be downloaded from the FAO's website (<https://www.fao.org/soils-portal/data-hub/>).
4. The soil map referenced in [27] was digitised with projections, converting it from a jpg format to a raster file.

2.5. Data Processing

2.5.1. DEM Processing

Following the preparation of the DEM layers for utilisation in ArcMap 10.3, we merged them into a novel raster format characterised by a resolution of 30 meters by 30 meters per cell. Subsequently, we proceeded to extract the designated area from the DEM raster. The resultant raster, thus generated, was employed in ArcGIS to delineate and construct the watersheds within the specified region.

2.5.2. Land Use/Land Cover Processing

In this study, the land use and land cover grid encompassing the entire watershed was obtained. Subsequently, the "Reclassify tool" within the Arc Toolbox's spatial analyst tools was employed. Through the reclassification process, the grid legend was transformed into a standardised category legend for further analysis and interpretation (Figure 3).

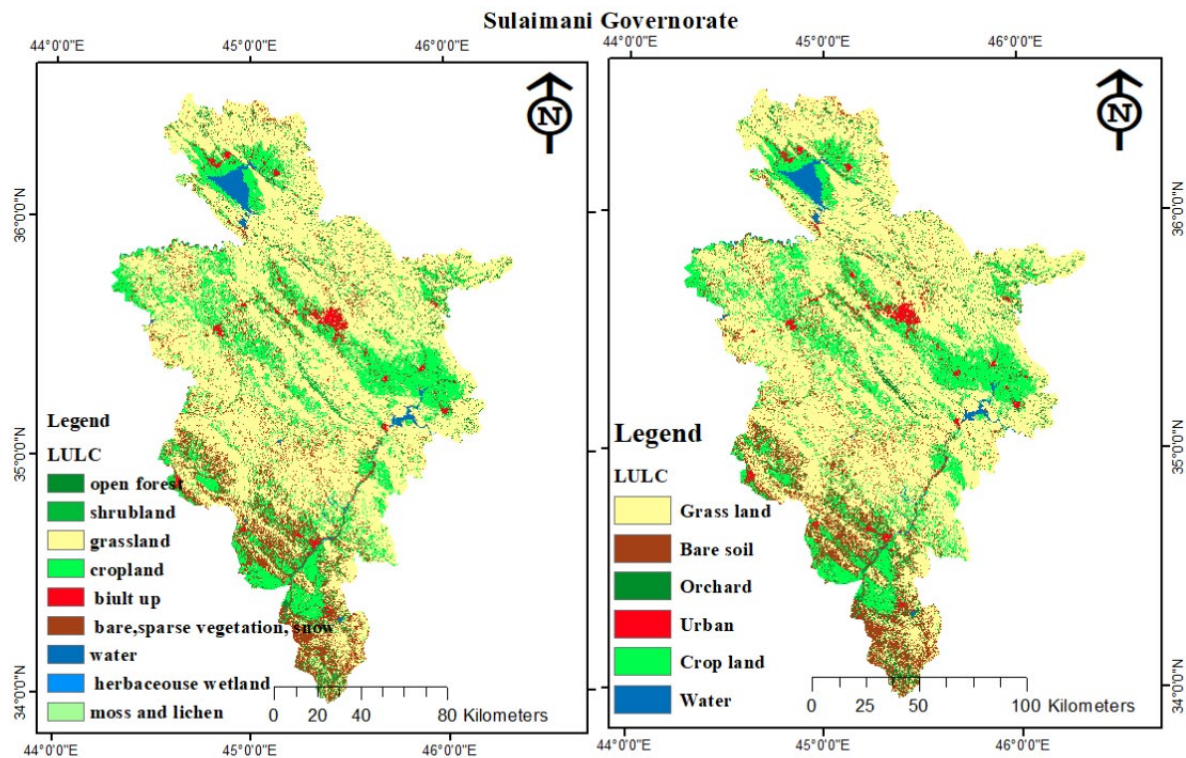


Figure 3: Land use and land cover processing; part (left) represents the original land use/land cover grid from ESRI, while part (right) represents the land use and land cover grid after reclassification.

2.5.3. Soil Data Processing

Using the appropriate shapefile delineating the study area and its corresponding watersheds, we extracted soil data raster information from the comprehensive global soil grid facilitated by the FAO. This raster dataset was subsequently transformed into the UTM-zone 38 coordinate system to ensure spatial alignment and consistency. The Harmonised World Soil Database (HWSD) Viewer (<https://www.fao.org/soils-portal/data-hub/>), served as the primary resource for accessing an array of soil properties, including gravel, clay, sand, silt percentages, and pH values, for depths up to one meter. A tabular presentation of attributes within the soil grid furnished detailed insights into various soil characteristics, such as predominant soil groups, types, textures, and unit names. Identification of soil types was facilitated through the utilisation of the NRCS online soil calculator (<https://www.nrcs.usda.gov/wps/portal/nrcs/detailfull/soils/>), which accounts for the proportions of silt, sand, and clay present in the soil composition. Moreover, expedited determination of the hydrological soil group was achieved through either the soil calculator or the HWSD Viewer, which provided comprehensive soil information. To establish the soil hydrologic group with precision, we juxtaposed the digitised Boringh map with the HWSD map. This synergistic approach yielded heightened accuracy in soil characterisation, culminating in the generation of an elaborate figure 4 elucidating the soil grid processing procedures within the study area.

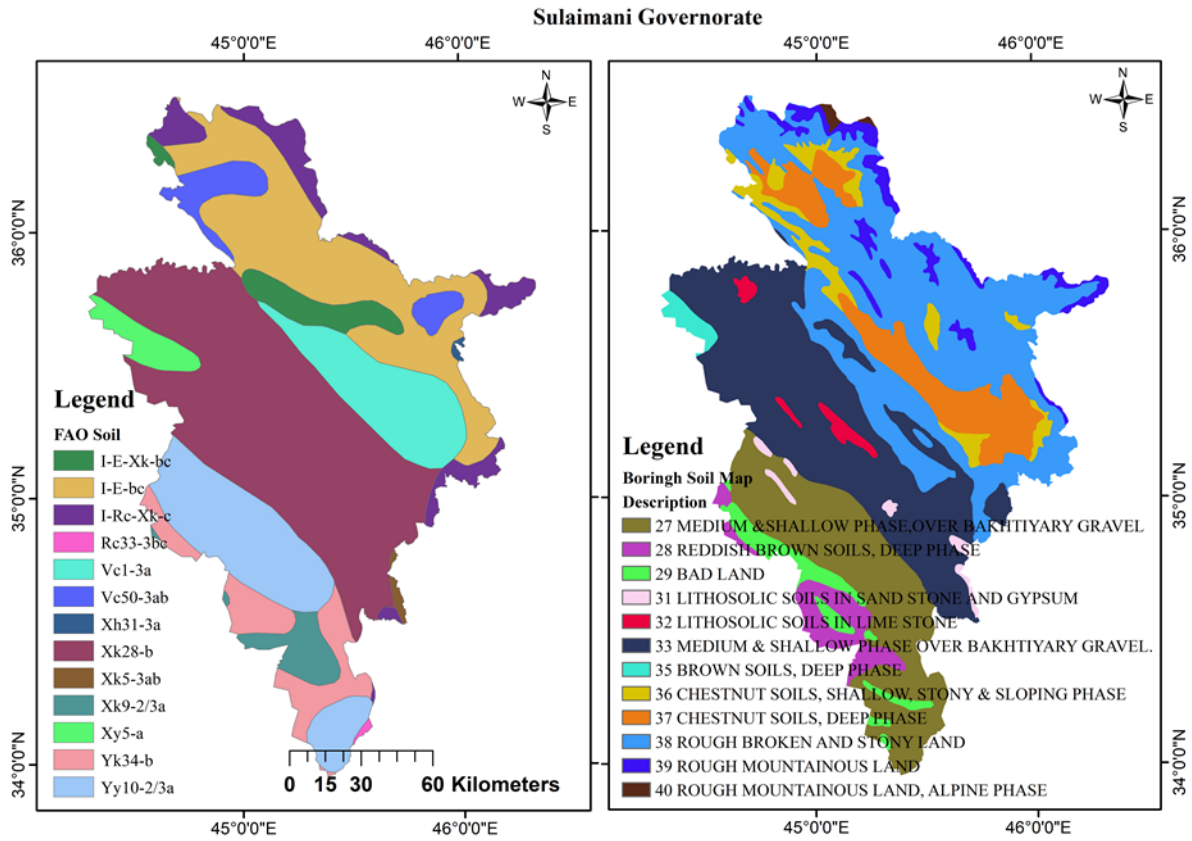


Figure 4: Soil data processing (Right) represents the clipped raster of the area under study from the Boringh soil map with the soil code that appeared in the legend of the map. (Left) denotes the clipped raster of the area under study from the original FAO soil map with the soil code that appeared in the legend of the map.

2.5.4 Generating the CN-II Map

To amalgamate the previously formatted grids, the "combine" tool within the "local" menu of Arc Toolbox's spatial analyst tools was employed. This tool facilitated the merging of the grids into a unified new grid, encapsulating all pertinent properties delineated within the LULC and soil data grids. Subsequently, within the composite layer, a new field was generated for tabular attributes. The assignment of CN values to each intersected feature was accomplished by referencing the CN-Lookup table delineated in the SCS-CN Methodology [28].

Table 3: Curve number value.

Land use, land cover type (LULC)	Hydrologic soil group			
	A	B	C	D
Urban	77	85	90	92
Agriculture	62	71	78	81
Bare soil	77	86	91	94
Orchard	43	65	78	82
Pasture	68	79	86	89
water	100	100	100	100

We performed a multiplication operation between the CN and the fraction of the entire watershed area to determine a weighted CN for each watershed. Equation 10 illustrates this calculation:

$$\text{weighted CN} = \frac{CN_1 \times a_1 + CN_2 \times a_2 + \dots + CN_n \times a_n}{a_1 + a_2 + \dots + a_n} \quad (10)$$

Where

CN₁, CN₂, CN_n refer to the curve numbers of the polygons.
 a₁, a₂, and a_n refer to the area of polygons.

2.6. Slope Adjusted Curve Number

The CN values listed in the NEH-4 table are primarily tailored for watershed slopes below 5%. However, it has been recommended by [21] to adjust these CN values when dealing with watershed slopes exceeding 5%. In response to this, [17] undertook a study in China, resulting in the development of Equations 11 and 12, specifically designed to adjust CNII values corresponding to varying watershed slopes.

$$CN_{IIadj} = CN_{II} \times K \tag{11}$$

$$K = \frac{322.79 + 15.63\alpha}{\alpha + 323.52} \tag{12}$$

Where

CN_{IIadj} = the curve number corrected for slope

For this study, we implemented a slope correction technique on the data utilised. The method recommended for slope correction applies to land slopes ranging from 14% to 140%.

2.7. Determining the Runoff Depth Adjusted for Slope

The slope-adjusted CN values, as previously discussed, were employed to determine the slope-adjusted runoff depth. Subsequently, we calculated the weighted runoff depth for each daily rainfall across the entire watershed, considering the slope factor.

3. Results

3.1. Rainfall Distribution and Topography Map

Variability in rainfall distribution is notable within Sulaimani governorate, situated in Iraq's Kurdistan region. Generally, the southern and southwestern sectors record lower annual precipitation levels, averaging around 165 mm. Conversely, as one progresses towards the northern and north-eastern territories bordering Iraq and Iran, precipitation rates escalate notably to approximately 1350mm additionally, the research zone displays diversity in terrain and slope characteristics. Southern areas exhibit fewer slopes, characterised by predominantly flat topography. Conversely, in the northern and north-eastern regions adjacent to the borders of Iraq and Iran, the prevalence of sloped land significantly increases, leading to much steeper terrain (Figure 5). These two factors are pivotal in influencing runoff dynamics.

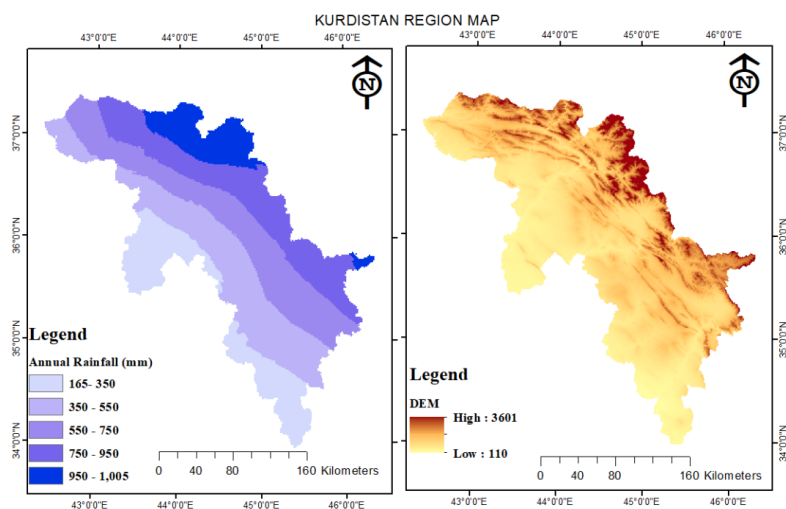


Figure 5: Variation of annual rainfall and topography in study area.

3.2. Hydrologic Soil Group

Figure 6 (left) illustrates a Geographic Information System (GIS) generated map depicting the hydrologic soil group distribution. Our analysis revealed the presence of all three hydrologic groups (B, C, and D) within Sulaimani governorate. Soils classified under Group B exhibited moderate infiltration rates, thereby indicating a moderate potential for runoff. Conversely, Group C soils displayed relatively low infiltration rates, resulting in a heightened potential for runoff. Meanwhile, Group D soils exhibited an elevated potential for runoff due to their notably low infiltration rates. Hydrologic soil Groups B, C, and D constituted 32.1%, 5.3%, and 62.6%, respectively, of the total study area.

3.3. Curve Number Value

Table 4 illustrates the CN values corresponding to each soil hydrologic group alongside their respective land use types. Hydrologic soil Group D exhibited elevated CN values, while Group B displayed lower CN values (Table 3). A study conducted in Argentina's humid temperate catchment observed a reduction in CN levels for hydrologic soil Group B. Similarly, research on creating the SCS-CN map for the Salt Creek watershed in northern Oklahoma reported CN values ranging from 100 (representing impervious land or water) to 58 (representing land with high infiltration, such as agricultural or forest areas).

In the Kurdistan region, urban areas and bare soil areas lacking developed soil layers (rocky terrain) are the primary contributors to runoff generation, as indicated in table 4. Figure 6 (right) showcases the CN value distribution within the study area, revealing that approximately 82.37% of cases had CN values ranging from 78 to 90. Moreover, 4.79% exhibited CN values below 78, while 12.83% had CN values exceeding 90. The map highlights that the southern and southwestern regions of Sulaimani governorate exhibit higher CN values compared to the north and northeast, attributed to lower annual precipitation and sparse vegetation cover. Research conducted in three rangeland watersheds in semi-arid northern Iran found that rangelands under poor and extremely degraded conditions displayed CN values higher than 85. It is worth noting that CN values are subject to variability and instability, and changes in land use can significantly influence watershed CN values.

Table 4: Curve numbers for different land uses and hydrologic soil groups in the Kurdistan region.

LULC	Hydrologic soil group	CNII	Area km ²	% LULC
Bare soil	D	94	2448.68	11.78
	B	86	298.73	
	C	91	111.54	
Crop land	D	81	3591.15	19.38
	B	71	682.89	
	C	78	430.97	
Grass land	D	89	8112.19	61.87
	B	79	6253.88	
	C	86	651.19	
Orchard	D	82	544.82	4.32
	B	65	480.48	
	C	78	23.52	
Urban	D	92	235.79	1.31
	B	85	55.16	
	C	90	29.16	
Water	B	100	19.57	1.34
	C	100	40.12	
	D	100	259.49	

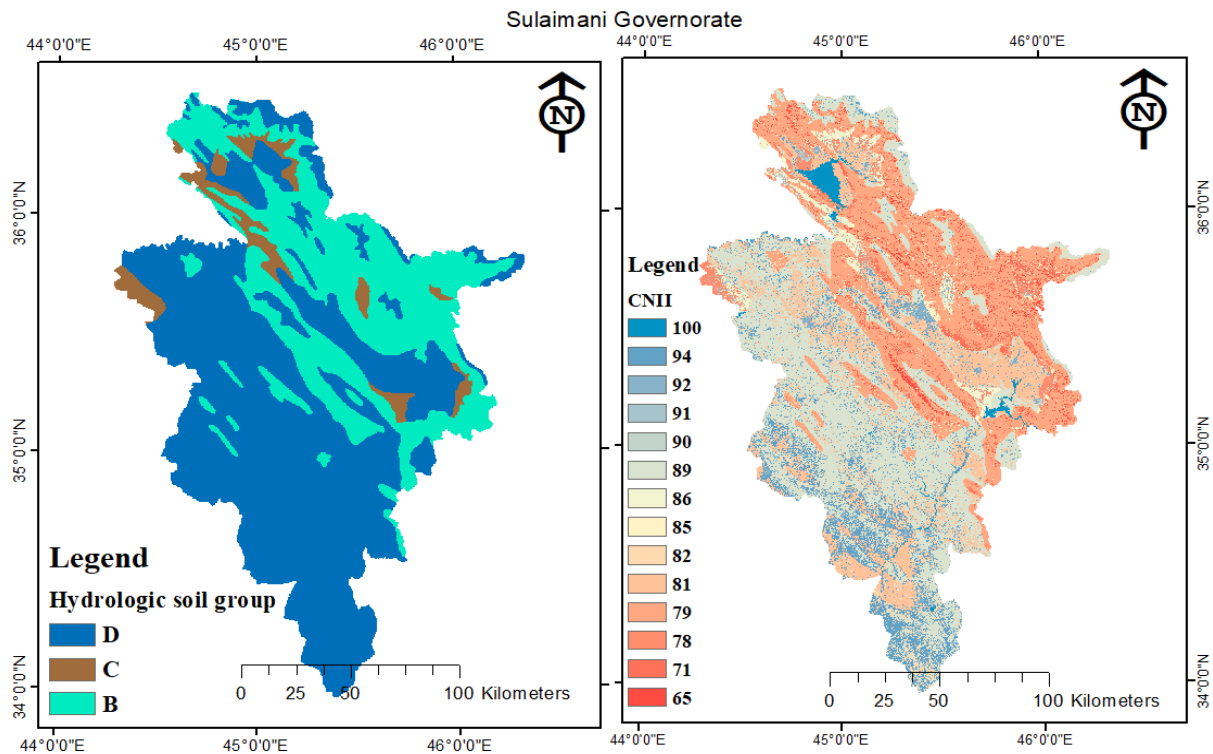


Figure 6: Sulaimani Governorate Hydrologic Soil Group and Curve Number (CNII) Map.

Following the delineation of seventeen watersheds across varied physiographic settings utilising DEM images, we extracted the CN watersheds from the primary CN map. Employing ArcGIS software, we computed the CN values for each watershed based on AMCII. Utilising Equations 8 and 9, we derived the CNI and CNIII values corresponding to AMC Class I and III, respectively. Table 5 illustrates that the lowest CN values were 57.06 and 88.99 (WS11), while the highest CN values were 77.88 and 95.90 (WS5) for CNI and CNIII, respectively. These findings suggest the presence of impermeable zones within the watersheds, likely attributable to the physical characteristics of rocks. Moreover, the region's limited vegetation cover contributes to elevated runoff rates. Table 5 further demonstrates that adjusting CNII for slope yields the most substantial alteration in CN value within the research region, particularly evident in WS5, characterised by a steep slope of 47.67%. In contrast, areas with a gentle slope of 5.94% (WS1) exhibit minimal changes in CN value following the adjustment of CNII for slope.

Table 5: Details of weighted curve number for watersheds of the study area and correction as per antecedent moisture conditions and adjusting slope.

Watersheds	CNI	CNII	CNIII	Slope	Slope (m/m)	K	Adj. slope CNI	Adj. slope CNII	Adj. slope CNIII
WS1	76.41	88.32	95.51	5.94	0.0594	1.0004	76.44	88.35	95.55
WS2	70.35	84.70	93.77	7.86	0.0786	1.0013	70.44	84.81	93.89
WS3	68.48	83.53	93.18	12.85	0.1285	1.0036	68.73	83.83	93.51
WS4	68.14	83.31	93.07	15.34	0.1534	1.0047	68.46	83.70	93.51
WS5	77.88	89.15	95.90	18.83	0.1883	1.0063	78.37	89.71	96.50
WS6	60.82	78.37	90.50	19.61	0.1961	1.0066	61.23	78.89	91.10
WS7	65.11	81.33	92.06	23.60	0.2360	1.0084	65.66	82.01	92.83
WS8	67.88	83.14	92.99	23.64	0.2364	1.0084	68.45	83.84	93.77
WS9	60.73	78.31	90.47	24.82	0.2482	1.0090	61.28	79.01	91.28

Table 5: Continue

WS10	64.48	80.91	91.84	27.70	0.2770	1.0103	65.14	81.74	92.78
WS11	57.06	75.62	88.99	27.74	0.2774	1.0103	57.65	76.40	89.90
WS12	63.70	80.38	91.56	41.74	0.4174	1.0166	64.76	81.71	93.08
WS13	59.97	77.76	90.17	44.71	0.4471	1.0179	61.04	79.15	91.78
WS14	60.06	77.82	90.20	45.13	0.4513	1.0181	61.15	79.24	91.84
WS15	63.52	80.25	91.50	45.56	0.4556	1.0183	64.68	81.72	93.17
WS16	62.13	79.29	90.99	45.91	0.4591	1.0185	63.28	80.76	92.67
WS17	71.01	85.11	93.97	47.67	0.4767	1.0193	72.38	86.75	95.78

3.4 Runoff Depth

The findings depicted in tables 6 and 7 reveal that in areas characterised by flat or very gentle slopes, the discrepancy in runoff depth before and after incorporating the slope factor is negligible. A comparison between the anticipated runoff depth without slope adjustment and the adjusted runoff depth demonstrates minimal variance. Essentially, table 5 underscores that modifying the CN values and integrating the slope factor equation (Equation 12) had marginal impact on runoff generation in flat or gently sloped terrains. However, as the slope gradient escalates, the CN values display greater variability, resulting in augmented estimated runoff subsequent to slope adjustment. Furthermore, the reduction from 0.2 to 0.1 in the λ yielded a substantial increase in runoff across all watersheds, both before and after adjusting the CN values for slope.

Table 6: Estimated runoff for watersheds before and after adjusting slope and modified initial abstraction ratio year (2021-2022).

Watersheds	Rainfall (mm)	$\lambda=0.2$		$\lambda=0.1$	
		Unadjusted slope	Adjusted slope	Unadjusted slope	Adjusted slope
		Runoff (mm)	Runoff (mm)	Runoff (mm)	Runoff (mm)
WS1	56.5	0.99	1.00	3.08	3.09
WS2	234.5	18.79	18.99	27.97	28.17
WS3	306.3	46.07	47.65	60.33	61.90
WS4	323.2	61.37	62.98	73.70	75.22
WS5	155.6	11.82	13.01	19.79	22.53
WS6	388.5	73.36	76.30	87.73	90.58
WS7	402.3	45.33	49.74	62.55	66.84
WS8	295.4	5.47	6.45	15.56	16.84
WS9	772.3	86.36	91.68	106.22	111.45
WS10	248	22.43	24.76	31.95	34.32
WS11	418.4	27.45	29.96	41.48	44.18
WS12	354.2	34.23	39.95	51.27	56.85
WS13	237.1	14.02	17.04	21.05	24.18
WS14	220.4	1.62	2.24	6.87	7.85
WS15	385	27.94	32.89	42.69	47.68
WS16	553	143.83	162.36	168.11	185.58
WS17	219.6	12.98	18.29	22.00	27.41

Table 7: Estimated runoff fore watersheds before and after adjusting slope and modified initial abstraction ratio year (2022-2023).

Watersheds	Rainfall (mm)	$\lambda=0.2$		$\lambda=0.1$	
		Unadjusted slope	Adjusted slope	Unadjusted slope	Adjusted slope
		Runoff (mm)	Runoff (mm)	Runoff (mm)	Runoff (mm)
WS1	312.5	6.43	6.47	16.66	16.72
WS2	429.5	42.39	42.76	64.76	65.18
WS3	438.4	20.31	21.10	42.45	43.45
WS4	453.9	28.09	29.21	51.22	52.58
WS5	381.0	18.40	19.71	18.40	19.71
WS6	803.2	152.25	155.96	203.98	207.76
WS7	593.8	38.54	42.08	63.91	67.66
WS8	689.0	67.10	70.61	100.52	104.47
WS9	778.5	108.51	112.35	156.07	158.92
WS10	670.0	13.34	14.98	31.94	34.15
WS11	606.2	61.01	64.24	89.10	93.15
WS12	640.0	93.42	105.51	126.99	138.71
WS13	456.9	13.39	16.58	34.72	38.74
WS14	443.4	11.79	14.72	29.53	33.15
WS15	720.2	92.54	105.86	126.06	138.97
WS16	523.3	7.99	10.13	27.07	30.38
WS17	539.7	72.59	86.12	106.45	120.49

3.5. Effect of Slope and Initial Abstraction Ratio on Runoff Generation

The impact of slope on runoff augmentation within a watershed exhibited variability, with its potency intensifying as the percentage of slope within the watershed increased. Upon scrutinising the effects of altering the λ and adjusting the CN for slope on runoff in watersheds, it becomes evident that modifying λ yields a significantly greater increase in runoff depth compared to adjusting the CN for slope. Results from the t-test indicated that altering the CN for slope and reevaluating λ exerted a substantial ($P \leq 0.01$) effect on the projected runoff, whether conducted independently or concurrently (Table 8). Furthermore, the findings indicated that elevating the slope CN elicited a relatively minor impact on runoff generation, both prior to and subsequent to modifying λ . However, when λ was adjusted to 0.1, the influence of slope on runoff quantity diminished compared to an initial abstraction ratio of 0.2.

Table 8: T-test results for estimated runoff before and after λ modifications and CN slope adjustment for the duration of the study.

#	factor	Comparison	t-value	DF	P	%95 Lower-upper
1	Modified initial abstraction ratio	Runoff predictions for year 2021–2022 before and after λ alteration without CN adjustment.	-9.055	16	0.000	(-15.15 to -9.383)
		Runoff predictions for year 2021–2022 before and after λ alteration with CN adjustment.	-9.563	16	0.000	(-15.046 to -9.586)
2	Adjust the curve number for the slope	Runoff predictions for year 2021–2022 before and after CN adjustment for the slope before altering λ .	-3.468	16	0.003	(-8.803 to -1.40)
		Runoff predictions for year 2021–2022 before and after CN adjustment for the slope after altering λ .	-3.797	16	0.002	(-5.712 to -1.619)

Table 8: Continue

3	Modified initial abstraction ratio	Runoff predictions for year 2022–2023 before and after λ alteration without CN adjustment for the slope.	-8.544	16	0.000	(-32.432 to -19.537)
		Runoff predictions for year 2022–2023 before and after λ alteration with CN adjustment for the slope.	-8.756	16	0.000	(-32.572 to -19.874)
4	Adjust the curve number for the slope	Runoff predictions for year 2022–2023 before and after CN adjustment for the slope before altering λ .	-3.877	16	0.001	(-6.396 to -1.874)
		Runoff predictions for year 2022–2023 before and after CN adjustment for the slope after altering λ .	-4.206	16	0.001	(-6.579 to -2.169)

4. Discussion

The usage of remote sensing technology in hydrological modelling has been increasingly recognised due to its distinct spatial data distribution. Various studies, such as those referenced by Nourani *et al.* [29] and Fry *et al.* [30] have extensively documented the integration of GIS into hydrological modelling practices. This integration involves leveraging satellite imagery, digital terrain data, LULC information, and hydrological soil groups data, all of which have become readily accessible over time. The NRCS-CN program, employed in distributed hydrological modelling, has seen a surge in usage over the past two decades, largely attributed to the proliferation of digital resources.

In our investigation, we harnessed remote sensing and geographic information systems to conduct an exhaustive analysis of rainfall distribution, topography, hydrological soil types, CN values, and runoff depths within the Sulaimani governorate of the Kurdistan Region in Iraq. Our findings unveiled considerable variations in rainfall distribution and topographical features across the region. The southern and southwestern sectors exhibited limited annual precipitation and relatively flat terrain, whereas the northern and north-eastern areas, bordering Iraq and Iran, experienced substantially higher rainfall and more rugged landscapes.

The hydrological soil group map generated through GIS delineated the presence of hydrologic groups B, C, and D within the Sulaimani governorate. Notably, our analysis indicated that hydrologic soil Group D exhibited elevated CN values, whereas Group B displayed diminished CN values. This trend mirrors findings observed by Gandini *et al.* [31] during their examination of hydrologic soil Group B within a humid temperate watershed in Argentina, which similarly led to reduced CN levels. Similarly, research conducted in the Salt Creek watershed in northern Oklahoma [32] resulted in the development of an SCS-CN map, showcasing CN values ranging from 58 to 100. These values corresponded to impermeable terrain and highly infiltrative land, respectively, underscoring the importance of land cover characteristics in runoff estimation. Furthermore, a study conducted in three semi-arid watersheds in northern Iran [33] delved into the assessment of rangeland conditions. Their findings revealed that rangelands characterised by poor and extremely degraded conditions exhibited CN values exceeding 85, highlighting the impact of land degradation on hydrological processes.

The SCS-CN model has gained widespread use for estimating watershed runoff during rainfall events due to its simplicity and minimal data requirements [1, 6]. However, as its popularity has grown, attention has turned to observations regarding slope and the initial abstraction ratio value. The CN values provided in the NEH-4 tables are typically suited for slopes of approximately 5% [22]. In the Kurdistan region, where terrain varies from relatively flat in the southwest to steeper in the northeast, assessing the model's predictive capability involved evaluating runoff both before and after adjusting the CN value for slope [17]. Similarly, studies by Mishra *et al.* [18] and Lal *et al.* [34] demonstrated that slope-corrected CN values led to significantly improved discharge predictions. The parameter λ , representing the initial abstraction ratio, has shown instability and variability across different geographic locations, often falling below the fixed threshold of 0.2 [35]. Research by Baltas *et al.* [35] in Attica, Greece, found an average ratio of 0.014, while Shi *et al.* [6] observed a range of 0.010 to 0.154, with mean and median values of 0.053 and 0.048, respectively. Yuan *et al.* [11] highlighted λ 's significant influence on runoff estimation, particularly in regions with low rainfall and semi-arid conditions. Additionally, Lal *et al.* [34] presented median and mean λ values of 0 and 0.034 for initial P-Q data and

0.033 and 0.108 for organised P-Q data. A recent study conducted by Abdulrahman and Karim [16] in the northeastern region of Kurdistan revealed variability in estimated λ values across different events, with over 92% falling below 0.2.

This study underscores the importance of slope and the initial abstraction ratio in the runoff formation process. Results indicate that the impact of slope on runoff increase varies and becomes more pronounced with higher percentages of slope in the watershed. Furthermore, altering the initial abstraction ratio (λ) has a more significant effect on increasing runoff depth than changing the slope CN.

5. Conclusions

To conclude, Sulaimani governorate exhibits notable disparities in rainfall distribution, with the southern areas receiving considerably less annual precipitation compared to the northern and northeastern regions. Additionally, the topography varies, characterised by flatter terrain in the south and progressively steeper slopes towards the north and northeast. These geographical features significantly influence runoff generation. The hydrologic soil groups present diverse characteristics across the region, with Group D predominating, indicating a high potential for runoff due to its limited infiltration rates. CN values display regional discrepancies, with lower values in the north and higher values in the south and southeast. Land use changes have a substantial impact on CN values, underscoring the importance of effective monitoring and management practices. When adjusting CN values for slope, a positive correlation between slope and runoff formation emerges, particularly in areas with more rugged terrain. However, the influence of slope on runoff formation is not as pronounced as the alterations in the λ . Decreasing the λ value leads to a more significant impact on runoff dynamics. Understanding the interplay between topography, soil characteristics, land use, slope-adjusted CN values, and modifications in the initial abstraction ratio is essential for precise runoff forecasting and effective watershed management in the Kurdistan region.

Authors contributions: Farhan Ahmad Abdulrahman: Data curation, Methodology, Writing – review & editing. Tariq Hama Karim: Formal Analysis, Investigation.

Data availability: Data will be available upon reasonable request.

Conflicts of interest: The authors confirm that there are no financial conflicts or personal connections that could potentially appear to bias the results discussed in this paper.

Funding: The authors did not receive support from any organization for the submitted work.

References

- [1] R. H. Hawkins, T. J. Ward, E. Woodward, and J. a Van Mullem, "Continuing evolution of rainfall-runoff and the curve number precedent," *2nd Jt. Fed. Interag. Conf.*, pp. 2–12, 2010.
- [2] Z. H. Shi, L. D. Chen, N. F. Fang, D. F. Qin, and C. F. Cai, "Research on the SCS-CN initial abstraction ratio using rainfall-runoff event analysis in the Three Gorges Area, China," *Catena*, vol. 77, no. 1, pp. 1–7, Apr. 2009, doi: 10.1016/j.catena.2008.11.006.
- [3] P. T. S. Oliveira *et al.*, "Curve number estimation from Brazilian Cerrado rainfall and runoff data," *J. Soil Water Conserv.*, vol. 71, no. 5, pp. 420–429, 2016, doi: 10.2489/jswc.71.5.420.
- [4] USDA-SCS, "Part 630 Hydrology National Engineering Handbook Chapter 10 Estimation of Direct Runoff from Storm Rainfall," *Natl. Eng. Handb.*, 1972.
- [5] M. Lal *et al.*, "Evaluation de la méthode du numéro de courbe du Service de la Conservation des Sols à partir de données provenant de parcelles agricoles," *Hydrogeol. J.*, vol. 25, no. 1, pp. 151–167, 2017, doi: 10.1007/s10040-016-1460-5.
- [6] Z. H. Shi, L. D. Chen, N. F. Fang, D. F. Qin, and C. F. Cai, "Research on the SCS-CN initial abstraction ratio using rainfall-runoff event analysis in the Three Gorges Area, China," *Catena*, vol. 77, no. 1, 2009, doi: 10.1016/j.catena.2008.11.006.
- [7] J. A. Reistetter and M. Russell, "High-resolution land cover datasets, composite curve numbers, and storm water retention in the Tampa Bay, FL region," *Appl. Geogr.*, vol. 31, no. 2, pp. 740–747, 2011, doi: 10.1016/j.apgeog.2010.12.005.
- [8] F. Fan, Y. Deng, X. Hu, and Q. Weng, "Estimating composite curve number using an improved SCS-CN method with remotely sensed variables in guangzhou, China," *Remote Sens.*, vol. 5, no. 3, pp. 1425–1438, 2013, doi: 10.3390/rs5031425.
- [9] M. Elhakeem and A. N. Papanicolaou, "Estimation of the runoff curve number via direct rainfall simulator measurements in the state of Iowa, USA," *Water Resour. Manag.*, vol. 23, no. 12, pp. 2455–2473, 2009, doi: 10.1007/s11269-008-9390-1.

- [10] D. E. Woodward, R. H. Hawkins, R. Jiang, A. T. Hjelmfelt, J. A. Van Mullem, and Q. D. Quan, "Runoff curve number method: Examination of the initial abstraction ratio," *World Water Environ. Resour. Congr.*, no. November 2018, pp. 691–700, 2003, doi: 10.1061/40685(2003)308.
- [11] Y. Yuan, W. Nie, S. C. McCutcheon, and E. V. Taguas, "Initial abstraction and curve numbers for semiarid watersheds in Southeastern Arizona," *Hydrol. Process.*, vol. 28, no. 3, 2014, doi: 10.1002/hyp.9592.
- [12] V. M. Ponce and R. H. Hawkins, "Runoff Curve Number: Has It Reached Maturity?," *J. Hydrol. Eng.*, vol. 1, no. 1, pp. 11–19, 1996, doi: 10.1061/(asce)1084-0699(1996)1:1(11).
- [13] M. Caletka, M. Š. Michalková, P. Karásek, and P. Fučík, "Improvement of SCS-CN initial abstraction coefficient in the Czech Republic: A study of five catchments," *Water (Switzerland)*, vol. 12, no. 7, pp. 1–28, 2020, doi: 10.3390/w12071964.
- [14] B. Randusová, R. Marková, S. Kohnová, and K. Hlavčová, "Comparison of cn estimation approaches," no. 7, pp. 34–40, 2015.
- [15] S. Kohnová, A. Rutkowska, K. Banasik, and K. Hlavčová, "The L-moment based regional approach to curve numbers for Slovak and Polish Carpathian catchments," *J. Hydrol. Hydromechanics*, vol. 68, no. 2, pp. 170–179, 2020, doi: 10.2478/johh-2020-0004.
- [16] F. A. Abdulrahman and T. Karim, "Reassessment of scs-cn initial abstraction ratio based on rainfall-runoff event analysis and slope-adjusted cn in a semiarid climate of halabja governorate," *Seybold Rep.*, vol. 18, no. 11, pp. 1391–1408, 2023, doi: 10.5281/zenodo.10276725.
- [17] M. Huang, J. Gallichand, Z. Wang, and M. Goulet, "A modification to the Soil Conservation Service curve number method for steep slopes in the Loess Plateau of China," *Hydrol. Process. An Int. J.*, vol. 20, no. 3, pp. 579–589, 2006, doi: DOI: 10.1002/hyp.5925 A.
- [18] S. K. Mishra, A. Chaudhary, R. K. Shrestha, A. Pandey, and M. Lal, "Experimental verification of the effect of slope and land use on SCS runoff curve number," *Water Resour. Manag.*, vol. 28, pp. 3407–3416, 2014, doi: 10.1007/s11269-014-0582-6.
- [19] D. S. Deshmukh, U. C. Chaube, A. E. Hailu, D. A. Gudeta, and M. T. Kassa, "Estimation and comparison of curve numbers based on dynamic land use land cover change, observed rainfall-runoff data and land slope," *J. Hydrol.*, vol. 492, pp. 89–101, 2013, doi: 10.1016/j.jhydrol.2013.04.001.
- [20] W. K. Dodds, "Distribution of runoff and rivers related to vegetative characteristics, latitude, and slope: a global perspective," *J. North Am. Benthol. Soc.*, vol. 16, no. 1, pp. 162–168, 1997, doi: 10.2307/1468248.
- [21] M. Ebrahimian, A. A. B. Nuruddin, M. A. B. M. Soom, A. M. Sood, and L. J. Neng, "Runoff Estimation in Steep Slope Watershed with Standard and Slope-Adjusted Curve Number Methods," *Polish J. Environ. Stud.*, vol. 21, no. 5, 2012.
- [22] A. N. Sharpley and J. R. Williams, "EPIC: The erosion-productivity impact calculator," *U.S. Dep. Agric. Tech. Bull.*, no. 1768, p. 235, 1990, [Online]. Available: <http://agris.fao.org/agris-search/search.do?recordID=US9403696>.
- [23] A. M. Melesse and S. F. Shih, "Spatially distributed storm runoff depth estimation using Landsat images and GIS," *Comput. Electron. Agric.*, vol. 37, no. 1–3, pp. 173–183, 2002, doi: 10.1016/S0168-1699(02)00111-4.
- [24] G. W. Musgrave, "How much of the rain enters the soil?," 1955.
- [25] A. T. Hjelmfelt Jr, "Empirical investigation of curve number technique," *J. Hydraul. Div.*, vol. 106, no. 9, pp. 1471–1476, 1980, doi: 10.1061/JYCEAJ.0005506.
- [26] S. K. Mishra, M. K. Jain, P. Suresh Babu, K. Venugopal, and S. Kaliappan, "Comparison of AMC-dependent CN-conversion formulae," *Water Resour. Manag.*, vol. 22, no. 10, pp. 1409–1420, 2008, doi: 10.1007/s11269-007-9233-5.
- [27] P. D. Buringh, "Soils and Soil Conditions In Iraq," *Minist. Agric.*, vol. 1, pp. 13–72, 1960.
- [28] S. K. Mishra and V. Singh, *Soil conservation service curve number (SCS-CN) methodology*, vol. 42. Springer Science & Business Media, 2003.
- [29] V. Nourani, V. P. Singh, and H. Delafrouz, "Three geomorphological rainfall–runoff models based on the linear reservoir concept," *Catena*, vol. 76, no. 3, pp. 206–214, 2009, doi: 10.1016/j.catena.2008.11.008.
- [30] L. M. Fry, T. S. Hunter, M. S. Phanikumar, V. Fortin, and A. D. Gronewold, "Identifying streamgage networks for maximizing the effectiveness of regional water balance modeling," *Water Resour. Res.*, vol. 49, no. 5, pp. 2689–2700, 2013, doi: 10.1002/wrcr.20233.
- [31] M. L. Gandini and E. J. Usunoff, "Curve number estimation using remote sensing ndvi in a GIS environment," *J. Environ. Hydrol.*, vol. 12, 2004.
- [32] H. K. Shukur, "Estimation curve numbers using GIS and Hec-GeoHMS ,odel," *J. Eng.*, vol. 23, no. 5, pp. 1–11, 2017, doi: 10.31026/j.eng.2017.05.01.
- [33] M. Nassaji and M. Mahdavi, "The determination of peak-flood using different curve number methods (case study, Central Alborze area)," *Iran. J Nat Resour*, vol. 58, pp. 315–324, 2005.
- [34] M. Lal, S. K. Mishra, and A. Pandey, "Physical verification of the effect of land features and antecedent moisture on runoff curve number," *Catena*, vol. 133, pp. 318–327, 2015, doi: 10.1016/j.catena.2015.06.001.
- [35] E. A. Baltas, N. A. Dervos, and M. A. Mimikou, "Technical note: Determination of the SCS initial abstraction ratio in an experimental watershed in Greece," *Hydrol. Earth Syst. Sci.*, vol. 11, no. 6, 2007, doi: 10.5194/hess-11-1825-2007.